Aircraft noise model improvement by calibration of noise–power–distance values using acoustic measurements

van der Grift, Rebekka; Snellen, Mirjam; Amiri-Simkooei, Alireza

DOI
10.1007/s13272-025-00902-6

Publication date
2025

Document Version
Final published version

Published in
CEAS Aeronautical Journal

CEAS Aeronautical Journal
https://doi.org/10.1007/s13272-025-00902-6

ORIGINAL PAPER

Aircraft noise model improvement by calibration of noise–power–distance values using acoustic measurements

Rebekka van der Grift[1] · Mirjam Snellen[1] · Alireza Amiri-Simkooei[1]

Received: 18 June 2025 / Revised: 29 August 2025 / Accepted: 29 September 2025

Abstract
To regulate aircraft noise impact on communities surrounding airports, best-practice models are used to predict aircraft noise levels. This research evaluates the noise–power–distance (NPD) tables employed in the European Doc 29 noise model using the noise measurements taken around Amsterdam Airport Schiphol. Thrust estimation is based on extracting the blade passing frequency from acoustic measurements and converting it to the engine rotational speed indicator $N1\%$. The $N1\%$ estimates are validated with onboard flight data. Even with accurate input parameters (thrust and distance to the observer), discrepancies are observed between modelled and measured noise levels, which can be attributed to the inaccuracies in the NPD tables. To further investigate this, empirical thrust-noise relations are derived from the measurements. These derived relations are found to differ from those in the original NPD tables. When the empirical thrust-noise relations are used, the agreement between the modelled and measured mean noise levels improves. The standard deviation of the differences gets reduced by 25% for departure operations. This finding is subsequently confirmed using independent measurements around Oslo Airport Gardermoen. Beyond improving current best-practice noise modelling, the methodology presented in this research offers insight into the development and validation of NPD tables.

Keywords Doc. 29 aircraft noise model · NOMOS measurement system · $N1$ estimation · Noise–power–distance tables · Noise measurements · Aircraft condition monitoring system (ACMS)

1 Introduction

The aviation industry is continuously growing, potentially resulting in increased noise exposure for communities surrounding airports. To investigate the effects of aircraft noise on these communities, predictive models have been established to calculate noise levels on the ground. These noise models are commonly used to regulate the number of operations or to create new flight routes to limit noise at specific times and locations. The models used for these applications are mainly (semi-)empirical models, i.e. based on measured data, with limited computational times, which is essential given the high volume of aircraft operations.

In Europe, a harmonised approach for noise modelling was deemed important. As such, the European Civil Aviation Conference (ECAC) developed the Doc 29 series of reports [1–3]. They present the methods for calculating aircraft noise following the current best-practice standards. This modelling framework, originally introduced in the 1970 s, has been periodically updated throughout the years to take newer aircraft models and new modelling insights into account. Similar to other best-practice noise models, such as the Aviation Environmental Design Tool (AEDT) [4] and the Dutch Noise Model (NRM) [5], Doc 29 makes use of Noise–Power–Distance (NPD) tables, which provide noise level data as a function of power (thrust delivered by engines) and the distance between the aircraft and the receiver. NPD tables provide multiple noise metrics for both approach and departure operations. This research focuses on two key noise metrics commonly used for noise contour calculations: $L_{A,\max}$, the maximum A-weighted overall sound pressure level, and Sound Exposure Level (SEL) [1].

✉ Rebekka van der Grift
r.c.vandergrift@tudelft.nl

Mirjam Snellen
m.snellen@tudelft.nl

Alireza Amiri-Simkooei
a.amirisimkooei@tudelft.nl

[1] Operations and Environment, Faculty of Aerospace Engineering, Delft University of Technology, Kluyverweg 1, 2629 HS Delft, The Netherlands

Published online: 25 October 2025

Both metrics are calculated per event, where SEL is used to calculate time-averaged levels such as L_{DEN}. The noise levels in the NPD tables are empirically determined through acoustic measurements and are standardised to the standard atmosphere and a reference speed of 160 kts, as specified in AIR-1845 [6]. These measurements are often acquired during certification practices and subsequently extrapolated to obtain entries for the full NPD table. Other models used for noise regulation, including the Swiss sonAIR model [7] and the German Anleitung zur Berechnung von Lärmschutzbereichen (AzB) [8], do not rely on NPD tables. Instead, they utilise more detailed spectral data and directivity patterns. A discussion of these models lies beyond the scope of this paper.

Studies related to the validation of models, such as Doc 29, have consistently reported differences between measurements and model predictions. Although the Doc 29 model is more often used for long time scales, such as yearly L_{DEN} calculations, validation studies for these metrics are limited. Reported discrepancies in L_{DEN} are on the order of at least 1 dBA when compared with measurements [9, 10]. Official documentation, AIR-1845, indicates a typical prediction accuracy of 1–2 dBA for locations directly beneath the flight path [6]. More commonly, however, the model is validated at the single-event level, where deviations can become larger [11–14]. Hogenhuis and Heblij [12] stated that such discrepancies may arise from uncertainties in the input parameters (thrust and weight) or from the current weather correction methods. To improve the model input, multiple methods have been proposed to retrieve thrust and weight from historical tracks, as an alternative to standard procedures [15, 16]. However, even with accurate thrust input, differences between predicted and measured noise levels will remain [17].

Rhodes and Ollerhead [13] argue that the differences are caused by the unavailability of NPD tables for certain aircraft types. Other studies have similarly identified such gaps in NPD tables as a possible source of error in noise modelling [18, 19]. To mitigate the contribution of this possible source of error, calibration of NPD tables has been proposed. For example, Sari et al. [20] used year-round long term noise measurements and L_{DEN} predictions to calibrate Doc 29. Trow and Allmark [21] presented a calibration method using single-event differences between model predictions and measurements. The aircraft thrust and position were modelled using procedural thrust profiles. The average difference from multiple flights was used to adjust the corresponding value in the NPD table. These corrections were then interpolated or extrapolated across the entire table. The disadvantage of this approach is that it is strongly affected by outliers. Although differences remained, the calibrated model was more accurate than the original model, and it altered the noise contour shapes [21].

The research objective of this paper aligns with the research described above, aiming to improve aircraft noise modelling by evaluating the Doc 29 input parameters and improving NPD tables using acoustic measurements. The main contributions of this paper are twofold. First, instead of estimating thrust from flight profiles, this study derives thrust directly from acoustic measurements, supported by actual flight data. Second, instead of adjusting the entries of the NPD table for each distance and thrust setting combination, the noise measurements are used to identify a relationship between thrust and noise level. These relations are then used to systematically update the NPD tables. The impact of this calibration method is investigated using noise measurements around Amsterdam Airport Schiphol (AMS) and Oslo Airport Gardermoen. Validation is accomplished using flight data from the Aircraft Condition and Monitoring System (ACMS). The updated NPD tables are used to improve noise modelling by reducing the mean prediction error and the standard deviation of the differences by 25%.

2 Data and methodology

In this research, measurements are used to validate and improve the Doc 29 model. For a fair comparison between the model results and measurements, accurate model input is necessary. To better understand the functioning and limitations of the Doc 29 model, an in-depth analysis of its input parameters is performed. Further, when comparing model results with measurements around Schiphol and Gardermoen airports, the characteristics and uncertainties of the microphone systems need to be accounted for. This section addresses these subjects in detail.

2.1 Schiphol NOMOS measurements

The Noise Monitoring System (NOMOS) encircling Schiphol Airport comprises 41 unattended continuous Noise Monitoring Terminals (NMTs) that have been operational since 1993. Each terminal is equipped with a class 1 microphone that has an uncertainty of 0.7 dB for elevation angles surpassing 60° [22]. They are mounted on poles ranging from 6 to 10 m in height and are distributed over various locations. Although primarily designed for public awareness, they are strategically positioned in and around communities, as depicted in Fig. 1 in relative xy-coordinates from the control tower at (0, 0). Detailed NMT locations are available on the NOMOS website.[1]

Not all NMTs are suited for research purposes, as placement near reflective surfaces or in regions with high

[1] https://noiselab.casper.aero/ams/.

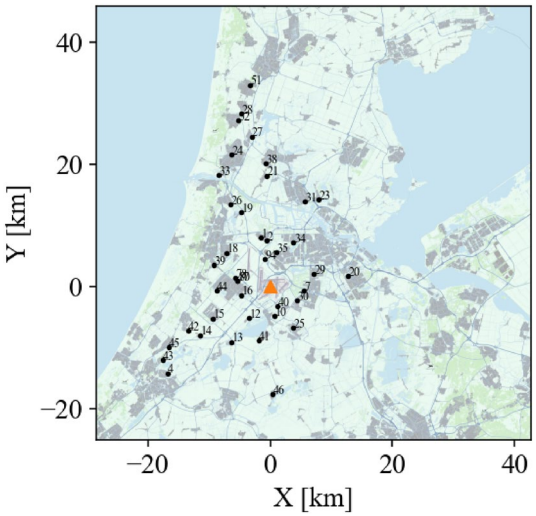

Fig. 1 Locations of NOMOS NMTs around Amsterdam airport Schiphol in xy-coordinates with respect to the control tower

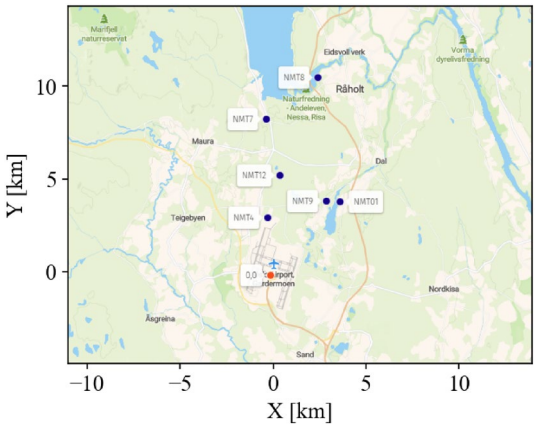

Fig. 2 Locations of the NMTs around Gardermoen airport

background noise can compromise the measurements. The NOMOS NMTs are tested against a set of validation criteria, such as the absence of reflective surfaces within 10 m and free from obstacles above a 20° elevation angle [23]. For the present study, only those NMTs that meet the validation criteria have been utilised. These stations record noise metrics for each event, particularly $L_{A,\max}$ and SEL, and also provide down-sampled (8000 Hz) mp3 files. For the latter, to avoid aliasing, a low-pass filter is applied to the original signal, eliminating all frequency content above 4000 Hz. For the research presented in this paper, $L_{A,\max}$ and SEL values are used to update the entries in the NPD table, while the mp3 files are used to derive $N1\%$ from the blade passing frequencies of the engines.

Most NMTs operate with a fixed 60 dBA threshold for $L_{A,\max}$, registering noise events that exceed this limit. To minimise the impact of background noise, only measurements with $L_{A,\max}$ >70 dBA are used for updating the NPD table. Furthermore, measurements with aircraft elevation angles $\beta > 60°$, relative to the NMT, are selected to reduce lateral attenuation and microphone uncertainties, aligning with ISO 20906 standards [24]. Additionally, only recordings taken under weather conditions compliant with ISO 20906, i.e. no precipitation and wind speed < 10 m/s, are considered in the analysis.

The measurement conditions explained above resulted in a dataset summarised in Table 1. The data cover all valid measurements from 2021 and 2022. This study focused specifically on the B737-800, the most common aircraft type flying at Schiphol. Other aircraft types, such as the A330-300 and the B777-300, were also analysed but are not discussed in detail in this paper.

2.2 Oslo measurements

To validate the findings around Schiphol, we also use measurements taken around Oslo airport, Gardermoen. Gardermoen Airport is equipped with 11 fixed NMTs, including a terminal at the end of the runway (NMT 4) and the rest in departure and/or arrival corridors. The area around Oslo is much less populated in comparison to Amsterdam. This results in lower background noise levels, down to 35 dBA for some NMTs. This makes most NMTs suitable for research purposes. The locations of these NMTs are illustrated in Fig. 2, again with respect to the local control tower.

The system used around Oslo has similar functionality and output to the NOMOS system. Due to the low background noise levels in this area, lower measured noise levels will remain reliable and a minimum threshold of $L_{A,\max} = 60$ dBA is taken. For consistency, similar requirements on operational conditions as those used for the NOMOS measurements are adopted here. An additional requirement is that the ground should be free of snow, as its cover significantly attenuates the measured sound. These criteria gave a set of measurements per NMT over the selected days in 2023, as presented in Table 2. This dataset is more limited than the one available for Schiphol. In particular, the arrival

Table 1 Number of considered measurements of the B737-800 per NOMOS NMT

NMT	1	10	12	14	21	30	34	40	41
Departures	–	1121	39	57	25	204	581	1725	114
Arrivals	1023	82	–	1314	24	–	–	–	–

Table 2 Number of considered measurements per Oslo NMT

NMT	1	4	7	8	9	12
Departures	9	2	47	28	5	45
Arrivals	–	–	–	93	–	–

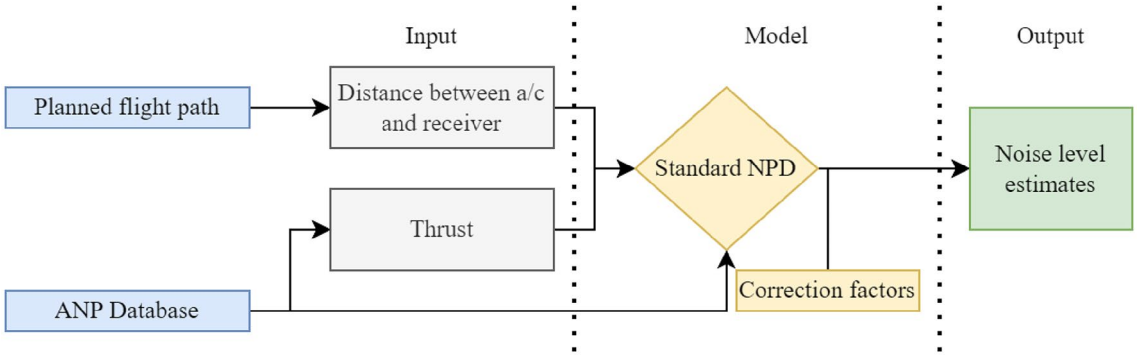

Fig. 3 Flowchart of input and output of the Doc 29 aircraft noise model

measurements are gathered from a single NMT, which can introduce bias.

2.3 Doc 29 model

The ECAC-developed Doc 29 provides detailed calculation instructions to model noise immission on the ground [2]. Doc 29 works similarly to other empirical models like the AEDT and NRM, which are also based on measurements.

Figure 3 provides a flowchart of the Doc 29 model. As mentioned, the model relies on NPD tables, which require two input parameters: engine power (thrust) and the distance between source and receiver. The distance can be determined accurately from the (expected) flight path of the aircraft, e.g. using positional data such as radar or ADS-B. The thrust estimation, however, is more difficult. For modelling planned operations, an estimation of the thrust profile is performed using so-called procedural steps. Each flight phase (e.g. take-off, climb-out) is associated with a given thrust setting. A few default procedures are available in the Aircraft Noise and Performance (ANP) database [25]. These procedures can differ by aircraft weight. The aircraft's weight is commonly estimated based on the expected distance that the aircraft has to fly and thus the associated fuel load. Despite ongoing research into thrust estimation from historical flight data, a lack of validated ground truth data will still remain. Thrust estimation methods based on aircraft performance require detailed information about the aircraft's weight and its aerodynamic characteristics. For example, Strümpfel and Hübner [15] used open-source Automatic Dependent Surveillance–Broadcast (ADS-B) data and the Base of Aircraft Data (BADA) [26] to achieve an 11% mean absolute deviation in thrust estimation. In this contribution, a different approach is adopted: thrust is directly derived from the acoustic measurements and consequently validated with flight data from the ACMS. The details of this method are given in Sect. 2.4.

The NPD tables are given for most aircraft types, but are often generalised. For example, the B737-700 and B737-800 make use of the same NPD table. To account for such variations, a general NPD correction factor is applied based on the configuration of the aircraft (i.e. engine-frame combination) using the EASA Type Certificate Database and its noise record number. These noise record numbers are given in the EASA Aircraft Noise Certificate (ANC) database or in national registers such as the Dutch aircraft register[2] for each specific aircraft tail number. The correction factor is a single offset in dBA applied uniformly to all NPD values, depending on whether the operation is departure or approach. Over the years, the introduction of newer and more efficient engines has led to changes in these correction factors. It should be noted that the levels in the NPD are for total aircraft noise, i.e., resulting from both engine and airframe noise, where the latter can be dominant during arrival [27].

The NPD tables are given for a set of standard conditions (right underneath the flightpath, ISA atmospheric conditions, etc.). For operations deviating from these standard conditions, additional correction factors are applied. These correction factors can significantly influence the calculated

[2] https://www.ilent.nl/onderwerpen/luchtvaartuigregister.

noise level. In this study, the correction factors used in Doc 29 are assumed to be accurate.

2.4 Thrust estimation from acoustic measurements

For Doc 29 and other best-practice methods, thrust is a key input parameter. Since thrust depends on many factors like the atmospheric conditions, flight path, and aircraft weight, an accurate method is required to derive the actual thrust at the time of the noise measurement. One effective method is to acoustically estimate the rotational speed of the engine using the recorded noise data [17, 28].

2.4.1 *N*1 estimation

Aircraft noise is a combination of airframe and engine noise. Airframe noise is typically broadband noise, while engine noise includes both broadband and tonal components [29]. The fan of the engine produces a tonal sound at the blade passing frequency (BPF) and its harmonics. The BPF is a function of the fan's rotational speed and the number of fan blades. The fan is connected to the low-pressure compressor, powered by the low-pressure turbine, or the $N1$ spool. The rotational speed of the engine is often expressed as a percentage ($N1\%$) of the maximum rotational speed ($N1_{\max}$). The $N1\%$ parameter is widely used by engine manufacturers and pilots to determine the engine delivered thrust [17]. The relation between $N1\%$ and the BPF is given by:

$$N1\% = \frac{60\,BPF}{n_{\text{blades}}\,N1_{\max}}100\% \tag{1}$$

where n_{blades} is the number of blades, and BPF is expressed in Hz.

To determine the BPF from the flyover audio recordings, the signal is segmented into one-second intervals and Fourier transformed. It is noted that the measurements contain ambient background noise. For the data considered in this paper, the background noise is considerably lower than the sound levels of the BPF tones. The BPF is estimated from the tones in the resulting spectrogram. Typically, both the fundamental BPF and its higher harmonics are visible in the spectrogram. For departing aircraft, which operate at high thrust settings, the range of 70–100% of maximum rotational speed $N1_{\max}$ is used to determine the BPF tones. Based on gathered flight data, this range has been shown to be appropriate for most aircraft during departure. An example spectrogram of a departure event is given in Fig. 4a.

Due to the Doppler effect induced by the relative motion of the aircraft, the frequencies of the received signals are shifted from those actually emitted. To eliminate these shifts, the spectrograms are de-Dopplerised using the

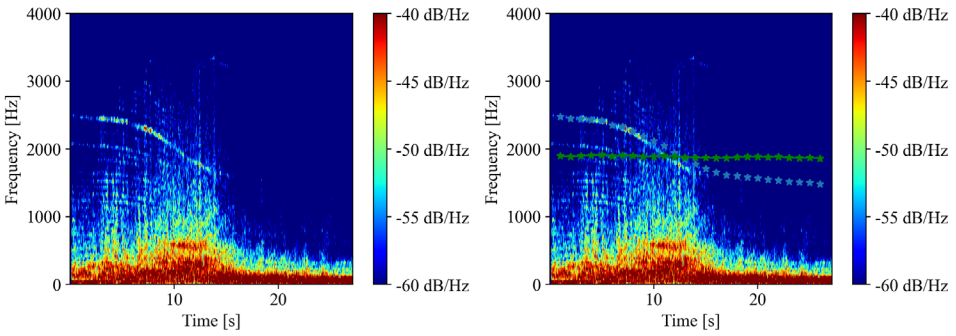

(a) Spectrogram of flyover measurement. (b) Estimated BPF (blue) and de-Dopplerised BPF (green).

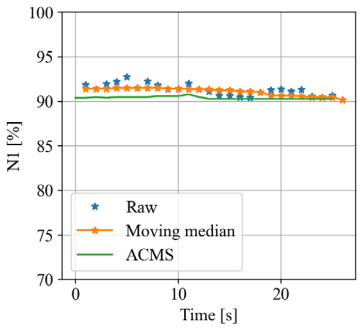

(c) Estimated $N1\%$.

Fig. 4 Results for $N1\%$ estimation and validation of a B737-800 departure flyover measurement

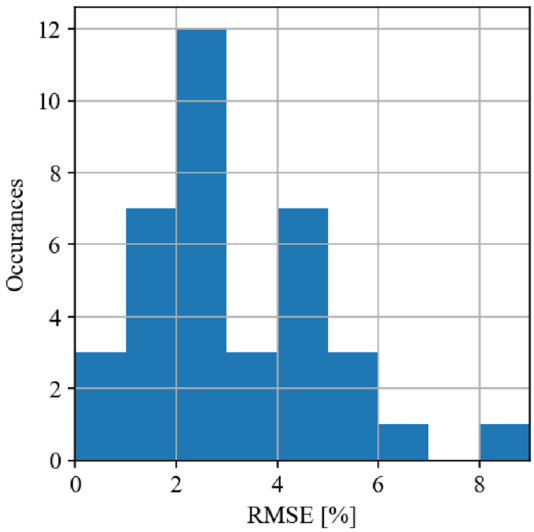

Fig. 5 Distribution of the root-mean-square error between the $N1$ estimation and the ACMS

aircraft positional information. In Fig. 4b, the detected BPFs are shown in blue for 1-s intervals, and the corresponding de-Dopplerised frequencies are shown in green. This method is described in detail by Merino-Martinez et. al.[17], and is based on the following relationship between the emitted frequency f and the Doppler-shifted frequency f':

$$\frac{f}{f'} = 1 + \frac{\mathrm{d}r/\mathrm{d}t}{c} \tag{2}$$

where $\mathrm{d}r/\mathrm{d}t$ is derived from the relative change of radial distance r between the NMT and the aircraft as obtained from the radar data, and c is the sound speed in air. To obtain a smooth temporal profile of the estimated BPF, a moving median filter is applied. This results in estimates for $N1\%$ as a function of time as seen in Fig. 4c.

As a validation step, the filtered $N1\%$ estimates are compared to those obtained from the ACMS data. The ACMS logs all important aircraft parameters, and is considered the golden standard for validation purposes [13]. Although not all measurements in this dataset meet the requirements mentioned in Sect. 2.1, e.g. the weather conditions or the 60-degree elevation angle requirement, they were nevertheless used for comparison with the limited ACMS data available. However, this is not expected to affect the results, since the validation concerns solely the frequencies at which tones occur, not their levels. A total of 37 departure measurements with corresponding ACMS data were available for the B737-800. The root-mean-square difference between the ACMS and spectrogram-derived $N1\%$, averaged over all 37 measurements, was found to be less than 4%. The distribution of this error over all flights is illustrated in Fig. 5.

For arriving aircraft, flight data indicated a rotational speed of roughly 30%. This results in a fan tone that is intertwined with the low-frequency background ambient and airframe noise, making the extraction of the BPF less reliable. Therefore, for arrivals, the tone corresponding to the first and second harmonics is used to determine the original BPF. Since arrival operations and flight paths are more stable and consistent than departure operations, the variation in $N1\%$ among arrival events is limited. From available arrival ACMS data, the B737-800 aircraft in the descent phase of the arrival operation flew a steady 29–33 $N1\%$, matching well with the values derived from the audio recordings.

2.4.2 Conversion of $N1\%$ to thrust

The last step to obtain the model input is to convert the estimated $N1\%$ values to corrected net thrust F_n/δ. The $N1\%$ to thrust conversion is not straightforward, as it depends on several additional parameters such as aircraft speed, ambient pressure and temperature [30]. The sonAIR model, developed by the Swiss research company Empa, uses $N1\%$ directly as input into the model without conversion to thrust, thereby removing this uncertainty [7]. Since Doc 29 still requires thrust input in pounds (lb), the conversion from $N1\%$ to thrust is necessary. An option is to use specific jet engine coefficients from the ANP database [25], which provides empirical relationships between $N1\%$ and thrust for various engine types. This relationship is typically expressed as [2]:

$$\frac{F_n}{\delta} = E_0 + F_0 V_C + G_A h + G_B h^2 + H T + K_3\left(\frac{N1\%}{\sqrt{\theta_T}}\right) + K_4\left(\frac{N1\%}{\sqrt{\theta_T}}\right)^2, \tag{3}$$

where E_0, F_0, G_A, G_B, H, K_3 and K_4 are constants derived from installed engine data. Further, δ is the pressure coefficient, V_c is the calibrated airspeed in knots, T is the ambient air temperature in Celsius, h is the altitude in *feet*, and θ is the ratio between ambient air temperature and standard reference temperature.

These coefficients are not available in the ANP database for most aircraft types. A recent study compares different methods for converting $N1$ to thrust [31]. They provided new ANP coefficients for the B737-800, which are given in Table 3, and will be used in the present study. It should be

Table 3 New ANP coefficients of the B737-800 taken from [31]

Method	E_0	F_0	G_A	G_B	H	K_3	K_4
Bounded LS	5260	− 15.77	− 0.0653	3.68e−07	− 5.934	− 172.5	3.661

noted, however, that these methods have not been validated for arrival operations. Given the relatively low thrust levels during arrival, small deviations may occur but are assumed to have a negligible effect on the results.

3 Model data comparison using standard NPD tables

3.1 Baseline data set using *N*1%

The baseline data set used in this research consists of roughly 3800 B737-800 departures from Schiphol Airport in 2021 and 2600 arrivals in 2022. These operations fall within the requirements stated in Sect. 2. As previously mentioned, the NOMOS provides measurements of both $L_{A,\max}$ and SEL, and hence model results will be compared against these parameters. For simplicity, only $L_{A,\max}$ will be presented in the plots. Figure 6a shows the NOMOS measured $L_{A,\max}$ levels for departure operations, plotted against the acoustically estimated $N1\%$ and the distance between the aircraft and NMT at the time of the measured $L_{A,\max}$. As expected, a clear inverse relation is observed between measured sound level and distance. A clear correlation between measured levels and engine setting is not immediately visible for the departure measurements. For arrivals, depicted in Fig. 6c, some influence of $N1\%$ on noise level is observed, though it remains difficult to see in the figures. The verification data set from Oslo airport is presented in Figs. 6b (departures) and 6d (arrivals). Similar patterns are visible as those observed in the Schiphol data set.

3.2 Difference in sound level between model and measurement

Figure 7 illustrates the measured $L_{A,\max}$ against that predicted by the Doc 29 model (with original NPD tables). The difference between the model and measured results is given by

$$\Delta L = L_{\text{model}} - L_{\text{measured}} \tag{4}$$

where a negative ΔL indicates an underestimation of the levels by the model. The agreement between model predictions and measurements is summarised in Table 4, where μ (indicating a bias) is the average difference between the model result and its corresponding measured values for all data events, and σ is the standard deviation of ΔL (indicating the precision). For both departure and arrival operations

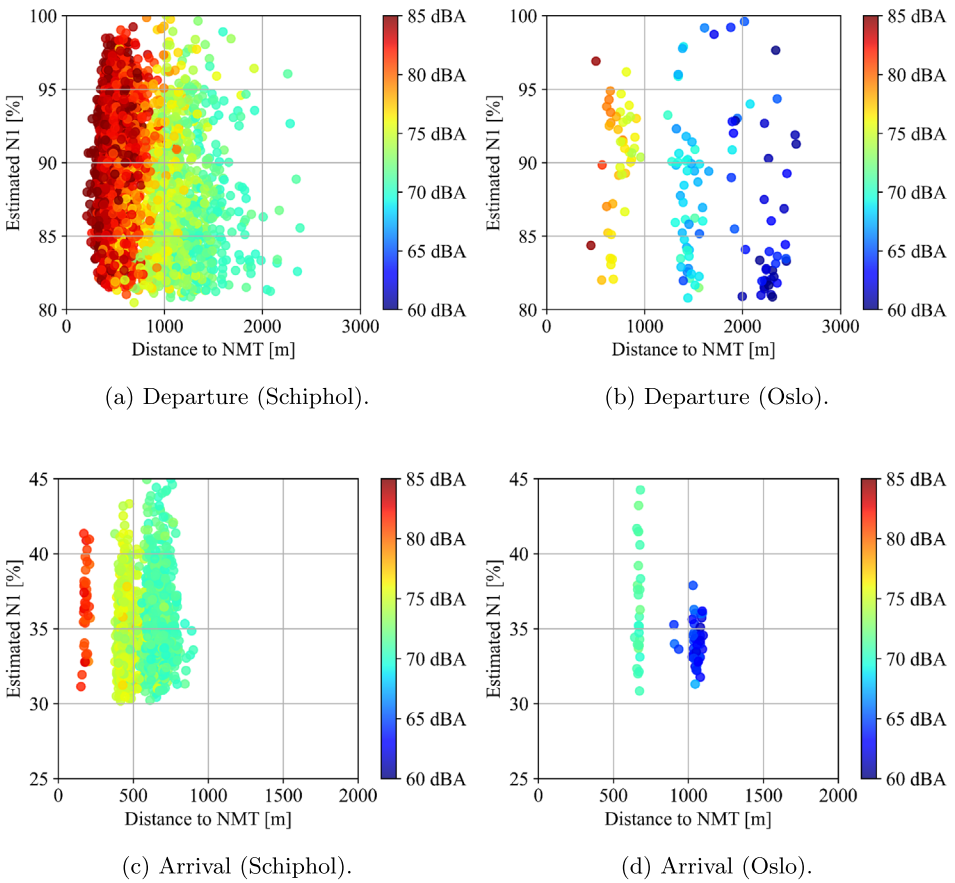

(a) Departure (Schiphol). (b) Departure (Oslo).

(c) Arrival (Schiphol). (d) Arrival (Oslo).

Fig. 6 Sound level of measurements ($L_{A,\max}$) for B737-800 as a function of distance and $N1\%$ for the baseline (Schiphol) and verification (Oslo) dataset

Table 4 Mean and standard deviation of the model results minus their corresponding measured values (mean and std. dev. of ΔL)

Airport	Operation	$L_{A,\max}$ [dBA]		SEL [dBA]	
		μ	σ	μ	σ
Schiphol	Departure	− 0.9	2.3	− 0.9	1.7
	Arrival	− 2.8	1.6	− 1.3	1.4
Oslo	Departure	− 0.5	2.5	0.0	2.1
	Arrival	− 1.7	1.4	− 0.7	1.4

at Amsterdam Airport Schiphol, the model underestimates the noise levels. The measured noise levels at Oslo airport in the verification data are lower, which is likely due to a lower background noise levels at those measurement locations, which in turn results in smaller underestimations. This holds true both for $L_{A,\max}$ and SEL values.

The results indicate differences between arrival and departure operations. For arrivals, a larger offset μ is visible, while the estimated standard deviations are relatively small. In contrast, departures exhibit a smaller offset but larger standard deviation. This larger variation in departure operations is consistent with findings in the literature [19, 32].

The arrival results are clustered around the NMTs, resulting in a small standard deviation. A clear spatial trend is observed: the offset appears to increase with distance from the runway. The larger the distance is (lower noise level), the larger the bias will be. The noise level is overestimated at NMT 10, while underestimated at NMTs 1 and 14. This can likely, in part, be explained by differences in approach speeds. At NMT 10, aircraft speeds are around 140 kts, compared to around 175 kts at NMT 14. The NPD tables have been calibrated for an approach speed of 160 kts, and apart from a modelled duration correction for SEL, no additional noise corrections are applied for speed differences. This duration correction is needed because SEL is an integrated metric, whereas $L_{A,\max}$ is a point metric. This would also explain the differences in results between $L_{A,\max}$ and SEL, as currently the $L_{A,\max}$ model predictions are independent of aircraft speed. A similar finding was recently reported during a validation study with the AEDT at San Francisco

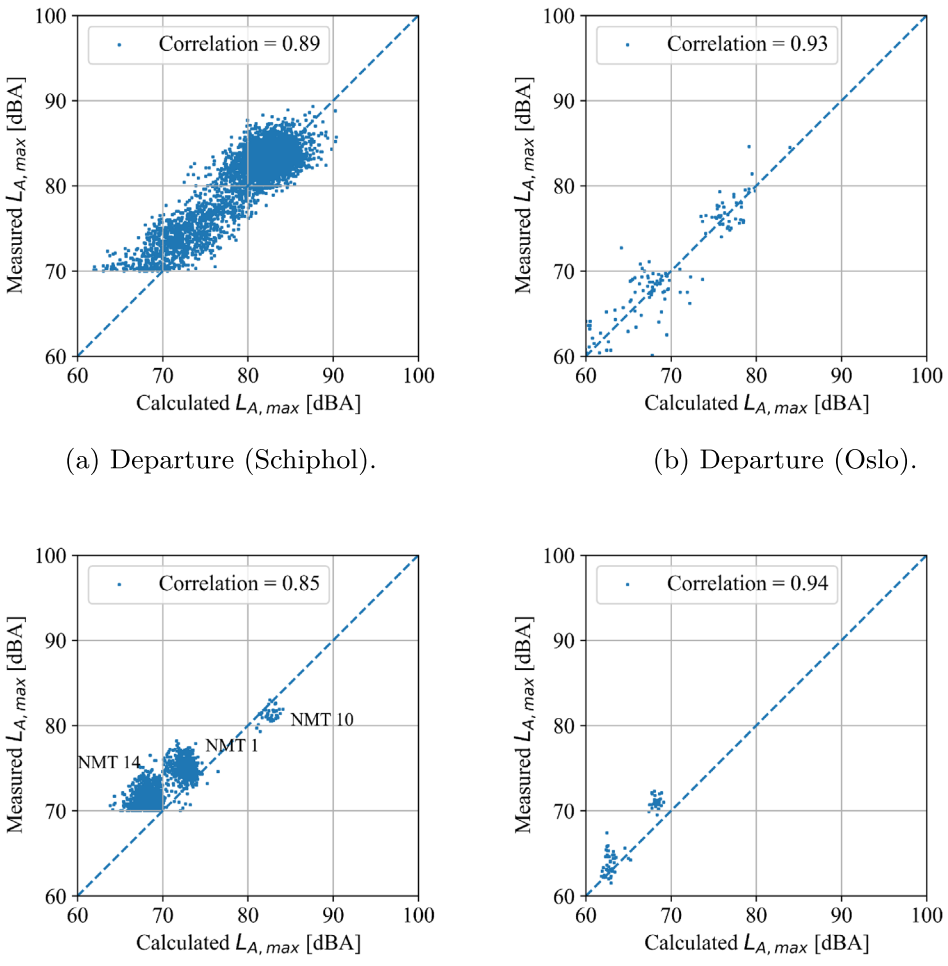

(a) Departure (Schiphol). (b) Departure (Oslo).

(c) Arrival (Schiphol). (d) Arrival (Oslo).

Fig. 7 $L_{A,\max}$ measurements of B737-800 with respect to Doc 29 model results (with original NPD tables), including corresponding correlation coefficient

Airport [33], where a 2.7 and 0.8 dBA underestimation is found for $L_{A,\max}$ and SEL, respectively. Although these speed-related observations are noteworthy, they fall outside the scope of this research.

To improve modelling results, the overall offsets can be reduced by implementing a general correction factor, such as the aircraft substitution correction factor. However, such corrections do not address the variation between modelled and measured values. To increase the accuracy and reliability of the model, this variation needs to be reduced.

To investigate the causes of these noise level differences ΔL, a correlation analysis is performed on the two main input parameters: distance and thrust. Although Pearson's correlation coefficient showed no significant relation between ΔL and distance, a strong correlation was found between the thrust and ΔL during departures. For arrivals, correlation with thrust was weaker but still present. Figure 8 illustrates the ΔL against the estimated thrust for both operations, where again a negative Δ indicates a model underestimation. The p-value for both results is smaller than 10^{-10}, indicating their statistical significance. These findings motivated a deeper investigation into the relationship between thrust and measured noise levels.

4 NPD table development

In this section, the relation between the measured noise levels ($L_{A,\max}$ and SEL) and the aircraft thrust is derived and compared with the current relation in the NPD table. The measured levels are back-propagated to the source by correcting for propagation effects. This is achieved by inverting the Doc 29 correction factors applied in the model, accounting for actual geometry and meteorological conditions during measurements.

For $L_{A,\max}$ measurements, these corrections are rather straightforward. The applied engine-frame model, ground impedance, engine installation and lateral attenuation corrections are inversely applied to the measurements. For the SEL measurements, however, this procedure is more complex. Unlike $L_{A,\max}$, SEL represents the integrated energy over multiple flight segments, each with distinct distances, thrust settings, speed and other correction factors. Since NOMOS provides only a single SEL value per event, the individual segment contributions to the total SEL are not directly available. In this study, an approximation is made: we assume that the correction factors for the measured segments are the same as those for the modelled segments, apart from a constant offset equal to the difference between the total measured and total modelled SEL. This approximation is then used to correct the measured SEL values. A sensitivity analysis (not shown here) conducted on a set of predicted and measured SEL values indicates that the uncertainty introduced by this approximation is limited to $\pm$ 0.3 dBA.

To correct the measurements for atmospheric effects, it is necessary to account for variations in weather conditions and measurement distances. These effects are frequency dependent. For the conversion of the measured values to those that would have been taken under standard atmospheric conditions, the frequency spectrum of the emitted sound needs to be accounted for. Using the frequency spectrum of the acoustic measurement, along with the corresponding meteorological data, the expected attenuation rates can be calculated. However, since NOMOS mp3 files are sampled with a sampling rate of 8000 Hz, the spectral information above 4000 Hz is not available. Therefore, the spectral information (also known as spectral classes) of the aircraft from the ANP database is used as a substitute. This use of spectral classes has been validated by van der Grift et al.[34].

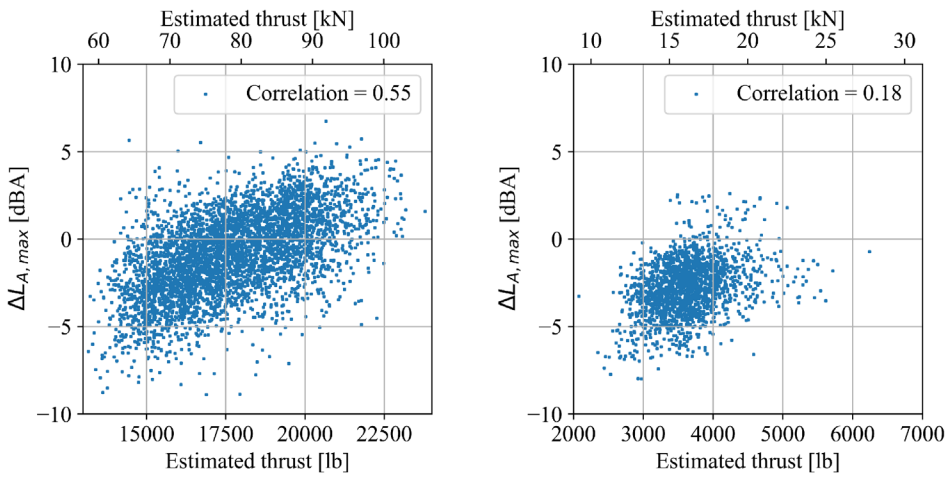

(a) $\Delta L_{A,max}$ for departures.

(b) $\Delta L_{A,max}$ for arrivals.

Fig. 8 The differences between model results and NOMOS measurements versus the estimated thrust (including corresponding correlation coefficient)

After applying all corrections and propagating the measurements to a reference distance of 1000 ft (305 m), the corrected noise levels are obtained at the reference distance. The relation between these levels and thrust is then made. This relation is illustrated in Fig. 9 for both departure and arrival measurements, and for both $L_{A,\max}$ and SEL. In general, the values derived from the NOMOS measurements and those documented in the NPD tables match within a couple of dBs. Previous studies indicate that the variation due to weather effects, next to atmospheric attenuation effects, can account for about 2 dB [35, 36], which partly explains the observed spread in the measurements. The other observation is that during departure operations, the measured noise level appears to depend less on the estimated thrust than originally assumed in the NPD tables. Assuming a measurement error (i.e. standard deviation σ_e) of 5 dBA, the 95% confidence interval for the slope of the fitted relation in Fig. 9b is $(3.9 \pm 1.2)10^{-4}$ dBA/lb. This dependence is thus statistically significant, which is also confirmed by the estimated correlation coefficient of 0.30 and a p-value of 10^{-27}). Figure 9a, b also show the thrust-noise level combinations based on thrust values obtained directly from the ACMS data, which further confirm the observed dependence. The slope estimated from the NOMOS data is approximately three times smaller than that of the NPD tables.

For the arrivals, the thrust-noise relation derived from the NOMOS data has a better alignment with the NPD table. Although thrust is generally assumed to be non-dominant during arrival, the NOMOS measurements show that the thrust setting is not insignificant and hence influences the measured noise levels. This is consistent with the findings of other studies on arrival measurements [37]. It is important to note that the thrust ranges differ significantly between

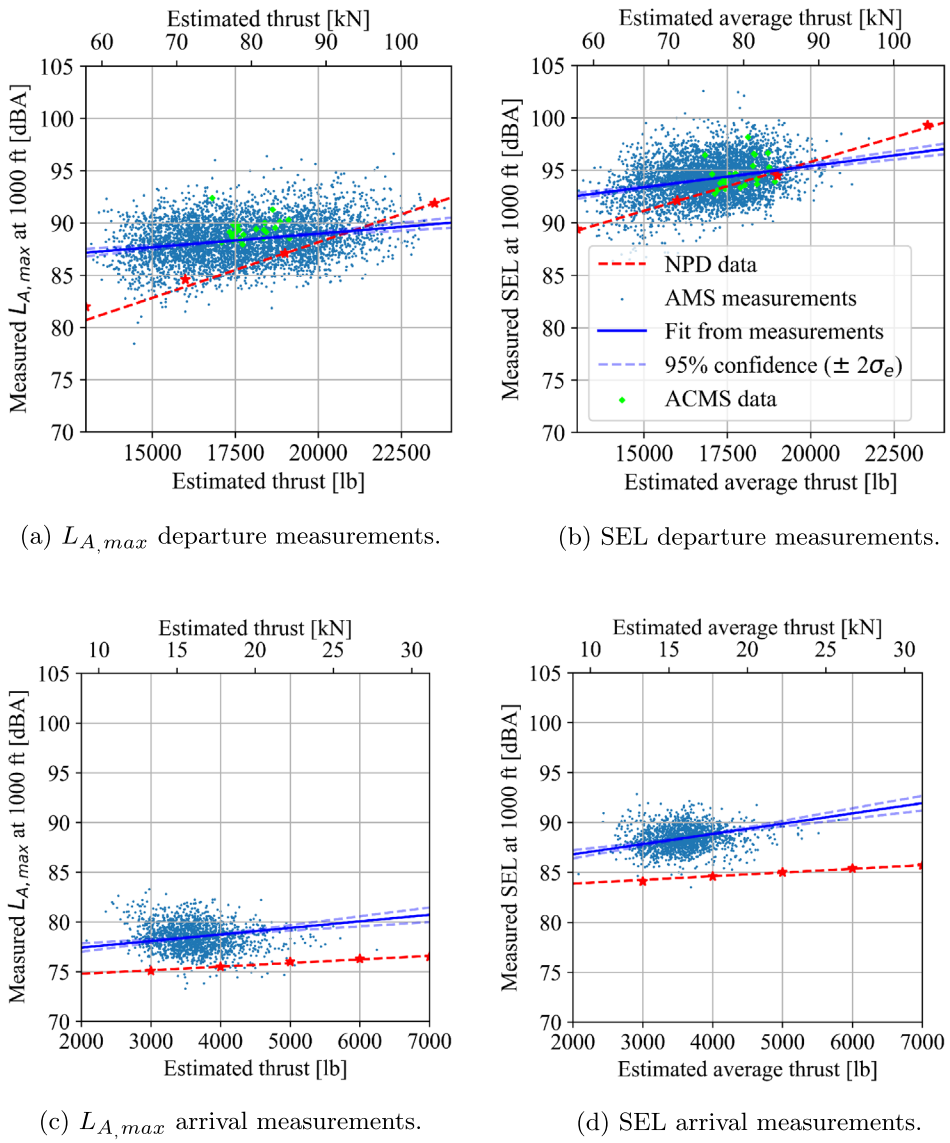

(a) $L_{A,max}$ departure measurements.

(b) SEL departure measurements.

(c) $L_{A,max}$ arrival measurements.

(d) SEL arrival measurements.

Fig. 9 Measurements of B737-800 standardised to a reference distance of 1000 ft. The graphs' legend is visible in the top right figure

the two operations: approximately 4000 lb for arrivals and 18,000 lb for departures.

To investigate whether the observed dependence in the departure measurements is consistent with other aircraft types, the analysis is repeated for the A330-300 and the B777-300ER, as seen in Fig. 10. Consistent with previous findings, the slope of the measured thrust-noise relation is smaller than that of the NPD data for both aircraft, although differences are visible between these two aircraft.

These insights are used to work towards modified NPD tables. Instead of calibrating the NPD values directly from measurements, the noise-thrust relations, such as those depicted in Fig. 9 are used to create completely new NPD tables. Each NPD table lists noise levels at ten reference distances in the range of 200–25,000 ft. For each distance, a thrust-to-noise level relationship is established using polynomial fitting. An example of such a fit at 1000 ft is illustrated in Fig. 9. The order of the polynomial is determined by validating the reduced chi-squared χ^2_ν statistic as a function of this polynomial order. Across all distances in this data set, the linear fit consistently provided the best results, which aligns with the current NPD assumptions that sound level increases linearly with thrust. This process results in ten linear fits, for which the noise levels at five thrust settings are extracted. This method leads to a new NPD table fully based on measurements and independent of existing NPD values. For the departure data set, it reveals a weaker dependence of noise on thrust compared to the original NPD table. Conversely, the arrival data set shows trends similar to the ones from the ANP database. There seems to be an even slightly stronger thrust-noise relationship.

A possible explanation for the above-described differences lies in the origin of the NPD tables themselves. Tables like that for the B737-800 were created during aircraft certification with the engine technology available at that time. Over the last 20–30 years, newer and hence quieter engines have been developed. A general correction factor, known as EASA aircraft substitution, is often applied to take this effect into account. This substitution correction factor tends to be small for arrival operations (typically around − 0.1 to − 0.2 dBA), but larger and more variable for departure operations, ranging from − 3 to + 0.5 dBA, depending on the specific engine type. This correction factor, however, is a single dBA value and does not capture changes in the thrust-noise relation due to newer engine technology. This can likely explain the large discrepancies observed between the modelled and measured noise-level changes with thrust during the departure operations.

5 Application of new NPD tables

5.1 Effect on single event measurements

To analyse the effect of using the new NPD table in Doc 29, the available data is split into a calibration and verification data set. The calibration data is used to establish the noise-thrust relations, and the verification data is subsequently used to validate the results. The data gathered around Schiphol airport is used for calibration, while the independent Gardermoen data is used for validation. The results are illustrated in Fig. 11a, b for the departures, and in Fig. 12a, b for the arrivals. The mean μ and standard deviations σ of the new results are given in Table 5.

We start with the calibration data set, where the results differ noticeably between departure and arrival operations. For the departure operations, the new method removes the small offset μ, but at the same time, the standard deviation

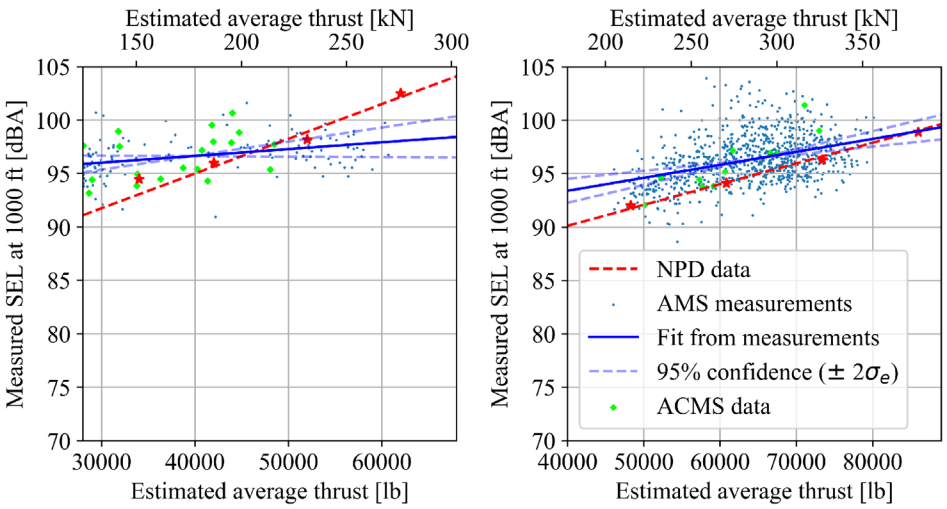

(a) SEL departure: A330-300.

(b) SEL departure: B777-300ER.

Fig. 10 SEL measurements of the A330 and B777 standardised to a reference distance of 1000 ft

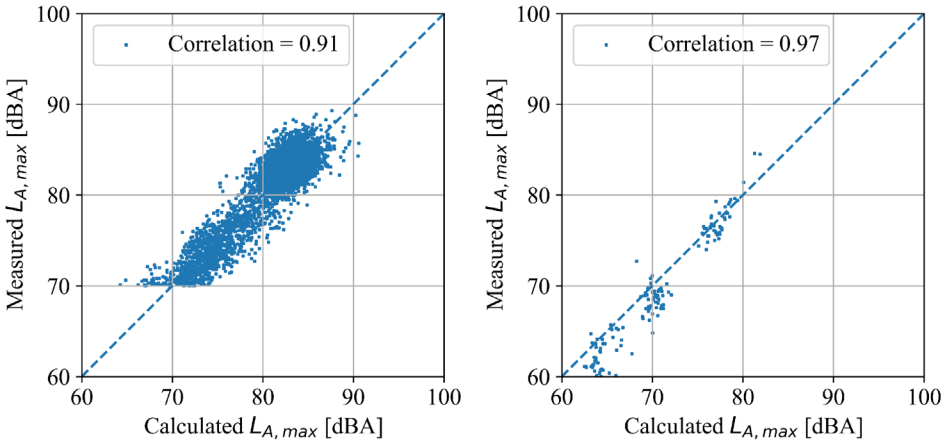

Fig. 11 $L_{A,\max}$ model results versus measurements of departure operations using new NPD tables (including the corresponding correlation coefficients)

(a) $L_{A,max}$ Schiphol calibration data set. (b) $L_{A,max}$ Gardermoen validation data set.

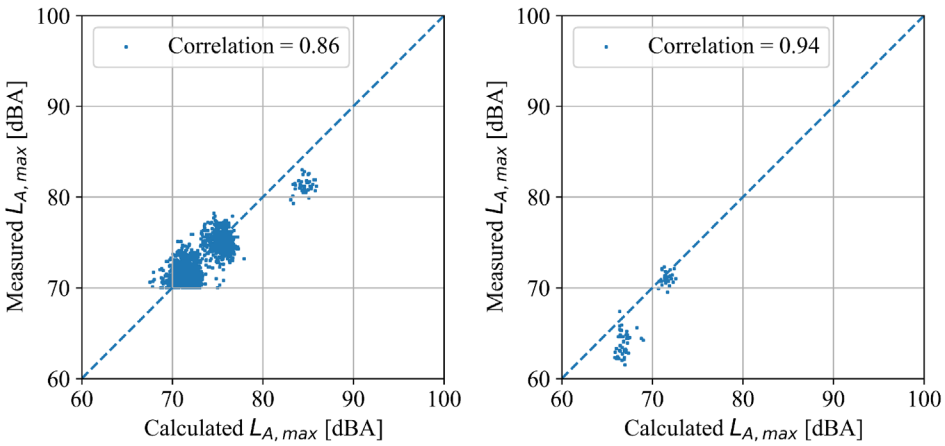

Fig. 12 $L_{A,\max}$ model results versus measurements of arrival operations using new NPD tables (including the corresponding correlation coefficients)

(a) $L_{A,max}$ Schiphol calibration data set. (b) $L_{A,max}$ Gardermoen validation data set.

Table 5 Results of ΔL for the model using standard and new NPD values

Operation	NPD	Data set	$L_{A,\max}$ [dBA]		SEL [dBA]	
			μ	σ	μ	σ
Departure	Standard NPD	AMS-calibration	− 0.9	2.3	− 0.9	1.8
		Oslo-validation	− 0.5	2.5	0.0	2.1
	New NPD	AMS-calibration	0.0	1.8	0.1	1.4
		Oslo-validation	1.3	1.6	0.4	1.5
Arrival	Standard NPD	AMS-calibration	− 2.8	1.6	− 1.3	1.4
		Oslo-validation	− 1.7	1.4	− 0.7	1.4
	New NPD	AMS-calibration	0.3	1.4	0.4	1.6
		Oslo-validation	2.0	1.6	1.6	1.3

decreased by 20–30%. This effect is also reflected in the correlation coefficient between model output and measurements, which increases for the departures. This indicates the accuracy improvement of the model results. In contrast, the arrival data set shows different behaviour. While the new NPD successfully removed the offset μ, it has minimal impact on σ. For arrivals, the new NPDs prove less effective at reducing the variation compared to their performance with the departure data set.

The validation data reveals a slightly different pattern. For both departure and arrival data sets, the offset μ of ΔL of the validation data is smaller than in the calibration data set when using standard NPD. However, the reduction in standard deviation at departures is as large as 30–35% when using the new NPD. This validates the model enhancement during the calibration. Arrivals present a contrasting outcome in the validation phase. The new NPD tables produce a large overshoot in the model predictions, and the previously low standard deviation even increases slightly. For the arrival operation, the new NPD tables therefore do not provide an improvement. A possible explanation is that NPD tables do not capture the variations in airframe noise at different operational phases, such as deployment of landing gear and high-lift devices. Further research is recommended on how to incorporate these components into best-practice noise models. In addition, the largest discrepancies between model predictions and measurements at Oslo occur at the lowest noise levels (< 70 dBA $L_{A,\max}$), which were discarded from the Schiphol dataset during the creation of the new NPD tables.

Despite this mixed performance across operation types, the method presented in this study produces more accurate model outcomes. When comparing the modelling methods, the new NPD, based on recent measurements instead of standard values, is a more dynamic approach to noise modelling.

5.2 Effect on SEL contour

Doc 29 is primarily used to calculate the aircraft noise impact on areas surrounding airports. This is done through calculations over a grid for numerous flights, creating, for example, L_{DEN} contours. In this contribution, we focus on the SEL contour for a single flight, using the flight path and $N1\%$ setting from ACMS data. As expected, applying the new NPD tables affects the resulting contour. Figure 13a shows the modelled SEL contour for a departure flight, while Fig. 13b illustrates the differences between the baseline model (using original NPD tables) and the updated model. Here, a negative ΔL (blue) indicates that the new model predicts a lower SEL value than the baseline model, while a positive ΔL (red) indicates a higher SEL value. The new NPD table results in lower predicted noise levels during the initial phase of the departure when high thrust levels are used. In contrast, higher predicted noise levels are observed at later stages in flight and at greater distances between the aircraft and the observer.

The arrival contour, not shown here, exhibits an overall increase in modelled noise due to the large offset present in the baseline model.

6 Conclusions

This paper presented a method to improve aircraft noise predictions by refining the input parameters and updating the Noise–Power–Distance (NPD) tables of the best-practice model Doc 29. In the first step, the uncertainty of the model input was reduced by using the flown track and acoustically derived thrust settings.

The second step involved the evaluation of the NPD tables currently in use. These NPD values were originally derived through (certification) measurements and are used in most best-practice methods. In this research, the NPD values were evaluated by comparing measured noise levels with model predictions that incorporate the actual thrust setting and distance, rather than relying on the default flight profiles. By minimising the errors in these input parameters, the remaining differences between model results and measurements (ΔL) can be attributed to inaccuracies in the NPD table. For the B737-800 data set, consisting of around 3800 departing and 2600 arriving flights, the offset μ was under 1 dBA for departures and 3 dBA for arrivals. The standard deviation σ of these differences was around 2 dBA and 1.5 dBA, respectively. Based on this analysis, a new NPD table was created from NOMOS measurements around Schiphol Airport.

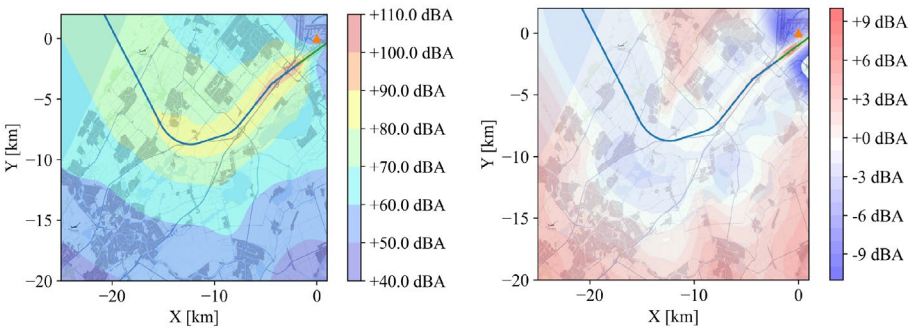

(a) Modelled SEL contour using standard NPD tables.

(b) Difference in SEL contour when using calibrated NPD tables.

Fig. 13 Difference in SEL contours between baseline and calibrated models for a departure operation

All measurements in the data set were standardised to the reference conditions used in the NPD tables. Several key insights emerged from this analysis. For the departure flights, the relation between thrust setting and sound level was less pronounced than originally expected. Incorporating these revised thrust-noise relations to create a new NPD table resulted in a 25% reduction in the standard deviation of differences between model and measurement. This improvement was consequently validated by applying the updated NPD tables on an independent data set at Oslo Gardermoen airport. For the arrival operations, different results were observed. The new NPD removed the offset μ between the measurements and the model results but did not reduce the standard deviation σ. This implies that the estimated thrust setting to noise ratio is not directly the cause of the differences seen between measurement and modelling results. Although updating NPD tables helps reduce the offset μ, further research is required to address the variation observed in the arrival aircraft noise prediction.

Although this research used data from Schiphol and Gardermoen Airport, the proposed methodology is applicable to any airport. While each airport has its own set of arrival and departure procedures, the NPD tables themselves are general and not airport-specific. To apply the methodology elsewhere, local thrust procedures must be validated. A limitation, however, is the need for validation data in the form of audio recordings ($N1$ estimations) or flight data. Once thrust is accurately determined, new NPD tables can be generated independently of the specific airport operation.

Measured thrust-noise relations, and consequently new NPD tables, can improve Doc 29 model predictions at the single-event level. Beyond improving the best-practice noise model, the methods described in this research give insight into the creation and validation of NPD values.

Acknowledgements This work was mainly supported by the Knowledge and Development Centre (KDC) Mainport Schiphol. The authors are also grateful to the EC for supporting the present work, performed within the NEEDED project, funded by the European Union's Horizon Europe research and innovation programme under Grant Agreement No. 101095754 (NEEDED). This publication solely reflects the authors' view and neither the European Union, nor the funding Agency can be held responsible for the information it contains.

Author Contributions R.G. conceptualized the research, worked on the data processing, methodology and validation. M.S and A.A. contributed to the methodology and supervision of the research. All authors contributed to writing, editing and reviewing of the manuscript.

Data Availability The data used for this research is not openly available.

Declarations

Conflict of interest The authors declare no conflict of interest.

References

1. European Civil Aviation Conference: Doc 29 report on standard method of computing noise contours around civil airports, 4th edition, volume 1: Applications guide. Technical report, ECAC. CEAC Doc29, Neuilly-sur-Seine Cedex, France (December 2016)
2. European Civil Aviation Conference: Doc 29 report on standard method of computing noise contours around civil airports, 4th edition report, volume 2: Technical guide. Technical report, ECAC. CEAC Doc29, Neuilly-sur-Seine Cedex, France (December 2016)
3. European Civil Aviation Conference: Doc 29 report on standard method of computing noise contours around civil airports, 4th edition, volume 3: Part 1—reference cases and verification framework. Technical report, ECAC.CEAC Doc29, Neuilly-sur-Seine Cedex, France (December 2016)
4. U.S. Department of Transportation Volpe National Transportation Systems Center: Aviation Environmental Design Tool (AEDT) Version 3f. Technical Manual. U.S. Department of Transportation, Washington, DC, USA (2023). U.S. Department of Transportation
5. Wal, H.M.M., Vogel, P., Wubben, F.J.M.: Voorschrift voor de Berekening van de Lden en Lnight Geluidbelasting in dB(A) Ten Gevolge van Vliegverkeer van en Naar de Luchthaven Schiphol. Part 1: Berekeningsvoorschrift
6. Society of Automotive Engineers: Procedure for the calculation of airplane noise in the vicinity of airports. SAE-AIR-1845A, SAE International, Warrendale, PA, USA (August 2012). https://doi.org/10.4271/AIR1845A
7. Jäger, D., Zellmann, C., Schlatter, F., Wunderli, J.M.: Validation of the sonAIR aircraft noise simulation model. Noise Map. **8**, 95–107 (2021). https://doi.org/10.1515/noise-2021-0007
8. Bundesministerium für Umwelt, Naturschutz und Reaktorsicherheit: Anleitung zur Berechnung von Lärmschutzbereichen (AzB). Bundesanzeiger, Nr. 195a vom 23.12.2008. Vom 19. November 2008 (2008)
9. Simons, D.G., Besnea, I., Mohammadloo, T.H., Melkert, J.A., Snellen, M.: Comparative assessment of measured and modelled aircraft noise around Amsterdam airport Schiphol. Transp. Res. Part D: Transp. Environ. **105**, 103216 (2022). https://doi.org/10.1016/J.TRD.2022.103216
10. Grift, R.C., Jayanthi, A.S., Amiri-Simkooei, A., Snellen, M.: Analysing the effect of undetected flights in the comparison of measured and modelled aircraft noise. In: 11th Convention of the European Acoustics Association (Forum Acusticum), Málaga, Spain (2025). European Acoustics Association
11. Rhodes, D.P., White, S., Havelock, P.: Validating the CAA aircraft noise model with noise measurements. Proceedings of Noise in London conference (2001)
12. Hogenhuis, R.H., Heblij, S.J.: Trendvalidatie van doc.29 berekeningen. NLR-CR-2017-371, Netherlands Aerospace Centre (NLR), Amsterdam, Netherlands (Oct. 2018)
13. Rhodes, D.P., Ollerhead, J.B.: Aircraft noise model validation. In: Proceedings of Inter-Noise, pp. 2556–2561 (2001)

14. Lepe, M., Lee, T., Huynh, J., Homola, M., Li, C., Hood, P., Hansman, R.J.: Multifactor analysis of operational factors contributing to aircraft overflight noise variation. In: AIAA Science and Technology Forum and Exposition, AIAA SciTech Forum 2025 (2025). https://doi.org/10.2514/6.2025-2004
15. Struempfel, C., Hübner, J.: Aircraft noise modeling of departure flight events based on radar tracks and actual aircraft performance parameters. In: Proceedings of DAGA 2020 46. Jahrestagung für Akustik (2020)
16. Behere, A., Lim, D., Li, Y., Jin, Y.C., Gao, Z., Kirby, M., Mavris, D.: Sensitivity analysis of airport level environmental impacts to aircraft thrust, weight, and departure procedures. In: AIAA Scitech Forum (2020). https://doi.org/10.2514/6.2020-1731
17. Merino-Martínez, R., Heblij, S.J., Bergmans, D.H.T., Snellen, M., Simons, D.G.: Improving aircraft noise predictions considering fan rotational speed. J. Aircr. (2018). https://doi.org/10.2514/1.C034849
18. Filippone, A.: Aircraft noise prediction. Prog. Aerosp. Sci. **68**, 27–63 (2014). https://doi.org/10.1016/j.paerosci.2014.02.001
19. Zaporozhets, O.: Aircraft noise models for assessment of noise around airports. Technical Report, ICAO environmental report (Sept. 2016). https://www.researchgate.net/publication/319159360
20. Sari, D., Ozkurt, N., Akdag, A., Kutukoglu, M., Gurarslan, A.: Measuring the levels of noise at the Istanbul Atatürk airport and comparisons with model simulations. Sci. Total Environ. **482–483**, 472–479 (2014). https://doi.org/10.1016/j.scitotenv.2013.07.091
21. Trow, J., Allmark, C.: The benefits of validating your aircraft noise model. In: Proceedings of Euronoise, 1269–1279 (2018)
22. Soede, W.: Technische beschrijving vliegtuig geluidmeetsystemen: Luistervink, nomos, sensornet. Technical Report 25971JGA1.016, ARDEA Acoustics and consult, Leiden, Netherlands (June 2012)
23. Sahai, A.R., Hogenhuis, R.N., Heblij, S.N., Smetsers, R.R., Verver, G.K., Assink, J.K.: Programmatische aanpak meten vliegtuiggeluid: Nationale meetstrategie. Technical report, National Institute for Public Health and the Environment Netherlands (RIVM) (July 2021). https://doi.org/10.21945/RIVM-2021-0001
24. International Organization for Standardization: Acoustics—unattended monitoring of aircraft sound in the vicinity of airports. Technical Report ISO 20906:2009, International Organization for Standardization (Dec. 2009). Reviewed and confirmed in 2020
25. European Union Aviation Safety Agency: Aircraft Noise and Performance (ANP) Data. https://www.easa.europa.eu/en/domains/environment/policy-support-and-research/aircraft-noise-and-performance-anp-data. Accessed: 2024-10-29 (2024)
26. Poles, D.: Base of aircraft data (BADA) aircraft performance modelling report. Technical Report EEC Technical/Scientific Report No. 2009-09, EUROCONTROL (Mar. 2009)
27. Bertsch, L., Snellen, M., Enghardt, L., Hillenherms, C.: Aircraft noise generation and assessment: executive summary. CEAS Aeronaut. J. **3**, 3–9 (2019). https://doi.org/10.1007/s13272-019-00384-3
28. Ramseier, T., Pieren, R.: Estimation of the fan rotational speed using flyover audio recordings. J. Aircr. **61**, 58–72 (2024). https://doi.org/10.2514/1.C037371
29. Vieira, A., Hoff, B., Snellen, M., Simons, D.G.: Comparison of semi-empirical noise models with flyover measurements of operating aircraft. J. Aircr. (2022). https://doi.org/10.2514/1.C036387
30. Deiler, C.: Engine thrust model determination and analysis using a large operational flight database. CEAS Aeronaut. J. **3**, 29–45 (2023). https://doi.org/10.1007/s13272-022-00625-y
31. Grift, R.C., Snellen, M., Amiri-Simkooei, A.: The effect of using $N1\%$ as input for aircraft noise modelling. Transp. Res. Part D: Transp. Environ. **142**, 104710 (2025). https://doi.org/10.1016/J.TRD.2025.104710
32. Giladi, R., Menachi, E.: Validating aircraft noise models. In: Proceedings of OpenSky Symposium, **59** (2020). https://doi.org/10.3390/proceedings2020059012
33. Rindfleisch, T.C., Alonso, J.J., Jackson, D.C., Munguía, B.C., Bowman, N.W., Ia, B.C.M.: A large-scale validation study of aircraft noise modeling for airport arrivals. J. Acoust. Soc. Am. **155**, 1928–1949 (2024). https://doi.org/10.1121/10.0025276
34. Grift, R.C., Snellen, M., Simons, D.G.: Validation of the aircraft noise and performance database source spectra. In: AIAA AVIATION 2023 Forum (2023). https://doi.org/10.2514/6.2023-3930
35. Simons, D.G., Snellen, M., Midden, B., Arntzen, M., Bergmans, D.H.T.: Assessment of noise level variations of aircraft flyovers using acoustic arrays. J. Aircr. **52**, 1625–1633 (2015). https://doi.org/10.2514/1.C033020
36. Heblij, S.J., Sindhamani, V., Arntzen, M., Bergmans, D.H.T., Simons, D.G.: Noise attenuation directly under the flight path in varying atmospheric conditions. In: Proceedings of Inter-Noise (2013)
37. Snellen, M., Merino-Martínez, R., Simons, D.G.: Assessment of noise variability of landing aircraft using phased microphone array. J. Aircr. **54**, 2173–2183 (2017). https://doi.org/10.2514/1.C033950